LETTERS

Accelerated ageing in mice deficient in Zmpste24 protease is linked to p53 signalling activation

Ignacio Varela[1]*, Juan Cadiñanos[1]*, Alberto M. Pendás[1], Ana Gutiérrez-Fernández[1], Alicia R. Folgueras[1], Luis M. Sánchez[1], Zhongjun Zhou[3]†, Francisco J. Rodríguez[1], Colin L. Stewart[4], José A Vega[2], Karl Tryggvason[3], José M. P. Freije[1] & Carlos López-Otín[1]

Zmpste24 (also called FACE-1) is a metalloproteinase involved in the maturation of lamin A (Lmna), an essential component of the nuclear envelope[1–3]. Both *Zmpste24*- and *Lmna*-deficient mice exhibit profound nuclear architecture abnormalities and multiple histopathological defects that phenocopy an accelerated ageing process[1,2,4,5]. Similarly, diverse human progeroid syndromes are caused by mutations in *ZMPSTE24* or *LMNA* genes[6–10]. To elucidate the molecular mechanisms underlying these devastating diseases, we have analysed the transcriptional alterations occurring in tissues from *Zmpste24*-deficient mice. We demonstrate that *Zmpste24* deficiency elicits a stress signalling pathway that is evidenced by a marked upregulation of p53 target genes, and accompanied by a senescence phenotype at the cellular level and accelerated ageing at the organismal level. These phenotypes are largely rescued in *Zmpste24*$^{-/-}$*Lmna*$^{+/-}$ mice and partially reversed in *Zmpste24*$^{-/-}$*p53*$^{-/-}$ mice. These findings provide evidence for the existence of a checkpoint response activated by the nuclear abnormalities caused by prelamin A accumulation, and support the concept that hyperactivation of the tumour suppressor p53 may cause accelerated ageing[11].

Alterations in nuclear envelope formation and dynamics are involved in the development of premature ageing syndromes. Thus, mice deficient in lamin A exhibit many features of premature ageing[4,5]. Similarly, disruption of the *Zmpste24* gene encoding a metalloproteinase involved in prelamin A processing causes nuclear architecture abnormalities[1,2], a shortened lifespan and multiple ageing-associated phenotypes[1,2] (Supplementary Fig. 1). The relevance of nuclear envelope alterations in accelerated ageing syndromes has been further confirmed by the finding that patients with different progeroid syndromes have mutations in *LMNA* or *ZMPSTE24* genes[6–10].

The availability of mice deficient in components of the lamin A–Zmpste24 system could provide new models to aid the study of mechanistic events underlying ageing in mammals. To this end, we first used oligonucleotide-based microarrays to analyse transcriptional alterations in tissues from *Zmpste24*-deficient (*Zmpste24*$^{-/-}$) mice. Out of 12,488 sequences present in the array and hybridized with RNA-derived probes from wild-type and knockout mouse liver, a total of 194 (1.6%) showed a higher than fivefold increase in expression levels in mutant versus control mice (Supplementary Table 1). By contrast, only 97 genes (0.8%) exhibited a greater than fivefold decrease in expression level in liver from *Zmpste24*$^{-/-}$ mice. Analysis of genes upregulated in the liver of *Zmpste24*$^{-/-}$ mice revealed that among the 25 genes for which expression was most upregulated, there were at least seven that have been characterized as downstream targets of the p53 tumour suppressor[12]. These p53 targets include *Gadd45a*, *p21* (also known as *Cdkn1a*), *PA26* (also known as *sestrin1*), *Btg2*, *Atf3*, *Rtp801* (also known as *Redd1* and *Ddit4*) and *Rgs16* (human synonym *A28-Rgs14*). Furthermore, in *Zmpste24*$^{-/-}$ mice there was also upregulation of other genes not identified as direct p53 targets but also associated with the p53 signalling pathway. These genes include *Gadd45b* and *Gadd45g*, which share multiple functional features with the p53 target *Gadd45a* in their response to DNA damage and other stresses[13]. The levels of observed upregulation of p53 target genes in *Zmpste24*$^{-/-}$ mice ranged from 31.8- to 9.1-fold for *Gadd45a* and *Btg2*, respectively. Northern blot analysis of liver RNAs from different *Zmpste24*$^{-/-}$ mice confirmed the upregulation of all these p53-inducible genes (Fig. 1a). Similarly, *in situ* hybridization experiments and western blot analysis of p21, a representative p53 target, provided additional evidence for the induction of a p53 response in the liver of *Zmpste24*$^{-/-}$ mice (Supplementary Fig. 2). Similar results were obtained after transcriptional profiling and northern blot analysis of heart from *Zmpste24*$^{-/-}$ mice, an organ severely affected by the deficiency of this metalloprotease[1] (Fig. 1a; see also Supplementary Table 1). We also detected expression differences of some p53 target genes between liver and heart from mutant mice, confirming the *in vivo* occurrence of tissue-specific induction of some p53 targets[14]: *Gadd45a* and *Rgs16* are upregulated in liver but not heart of *Zmpste24*$^{-/-}$ mice (Fig. 1a), whereas *Igfbp3* is upregulated in heart but not liver (Fig. 1b). We also observed a marked degree of variability in the levels of induction of p53 targets depending on the severity of phenotype of *Zmpste24*$^{-/-}$ mice. Thus, mutant mice showing the most advanced progeroid signs consistently had the highest expression levels of p53 targets (Supplementary Fig. 3).

Parallel experiments performed with liver from mice deficient in lamin A, the Zmpste24 substrate, also revealed upregulation of p53 transcriptional targets (Fig. 1a; see also Supplementary Table 1). Nevertheless, despite the marked upregulation of p53 target genes in tissues from *Zmpste24*$^{-/-}$ and *Lmna*$^{-/-}$ mice, western blot analysis did not reveal an increase in p53 protein levels in any of them (Fig. 1c), as previously described in senescence-associated processes[15]. We next explored whether a putative p53 isoform present in *Zmpste24*$^{-/-}$ cells could be responsible for the upregulation of p53 target genes, but we did not observe any alternatively spliced form of p53 in *Zmpste24*$^{-/-}$ mice (Supplementary Table 2). Similarly, we did not observe variations in the status of p53 phosphorylation at Ser 18 and Ser 23, two post-translational changes that activate p53 function[16] (Fig. 1c). We also failed to detect acetylated p53 in liver from mutant mice (data not shown). Therefore, it seems that common

[1]Departamento de Bioquímica y Biología Molecular, Facultad de Medicina, Instituto Universitario de Oncología, and [2]Departamento de Morfología y Biología Celular, Universidad de Oviedo, 33006 Oviedo, Spain. [3]Division of Matrix Biology, Department of Biochemistry and Biophysics, Karolinska Institutet, Stockholm S-17177, Sweden. [4]National Cancer Institute, Frederick, Maryland 21702, USA. †Present address: Department of Biochemistry, Facult of Medicine, University of Hong Kong, Pok Fu Lam, Hong Kong.
*These authors contributed equally to this work.

post-translational modifications are not involved in the p53 activation mechanism probably responsible for the upregulation of several targets of this tumour suppressor in *Zmpste24*$^{-/-}$ mice. Further studies revealed that levels of phosphorylated histone H2AX—an early marker of cell response to DNA damage—are increased in liver from *Zmpste24*$^{-/-}$ mice (Fig. 1d), indicating the occurrence of a DNA damage response in these mice that could lead to p53 activation. These results agree with recent findings showing genomic instability in laminopathy-based premature ageing[17]. Taken together, the above results are consistent with the hypothesis that the nuclear abnormalities occurring in mice deficient in the lamin A–Zmpste24 system trigger a stress response linked to the activation of a signalling pathway involving p53 transcriptional targets.

To evaluate the possibility that structural abnormalities emanating from the nuclear envelope defects observed in *Zmpste24*$^{-/-}$ cells[1] could be sensed as p53-activating signals, we performed an ultrastructural analysis of tissues from mutant mice. This analysis revealed profound chromatin alterations in *Zmpste24*$^{-/-}$ cells (Supplementary Fig. 4), which could evoke the genotoxic stress that elicits a p53-mediated response and leads to cellular senescence or death by apoptosis[18]. To analyse further the p53-linked response induced in *Zmpste24*$^{-/-}$ mice, we examined whether cells from these mutant mice enter senescence earlier or undergo apoptosis at a higher rate than control cells. Cell senescence is associated with a spontaneous decline in growth rate and a terminal arrest of the cell cycle[19,20]. Therefore, we first performed a comparative analysis of the proliferative ability of primary fibroblasts from these mice and their wild-type littermates. As shown in Fig. 2a, fibroblasts from 12-week-old *Zmpste24*$^{-/-}$ mice exhibited a marked proliferative decrease when compared with control cells. This decrease was not primarily caused by an increased sensitivity to culture stress, as it was maintained under reduced (3%) oxygen conditions (Fig. 2b). To analyse the effect of *Zmpste24* deficiency on cell cycle, we measured the percentage of replicative cells in fibroblast cultures after 5-bromodeoxyuridine (BrdU) exposure (Fig. 2c). Whereas 15.5% of control cells were positive, only 6.3% of the *Zmpste24*-deficient fibroblasts incorporated the nucleotide analogue. Accordingly, the percentage of cells in S phase was lower in the absence of Zmpste24, increasing the fraction of cells both in G1 and G2/M phases (Fig. 2d). Therefore, *Zmpste24*$^{-/-}$ fibroblasts show a reduced proliferative activity that apparently derives from the lower replicative capacity of these cells.

In addition to growth arrest, senescence is associated with a series of distinctive molecular and morphological alterations[19–21]. Analysis of the putative occurrence of features characteristic of senescent cells in *Zmpste24*$^{-/-}$ mice showed that *Zmpste24*$^{-/-}$ fibroblasts displayed flattened and enlarged morphology, and were positively stained for β-galactosidase at pH 6.0, a biological marker of senescent cells[19] (Fig. 2e). Histochemical analysis of kidney sections from *Zmpste24*$^{-/-}$ mice also revealed a strong β-galactosidase activity at pH 6.0 (Fig. 2e). We also observed a marked upregulation of secretory factors—including proteases such as cathepsin L—that may disrupt tissue integrity and function, and are associated with the development of senescence phenotypes[20] (Fig. 2f). Despite shortened telomere length being associated with senescence[22], no significant differences in telomere length were found between wild-type and *Zmpste24*$^{-/-}$ mice (A. Canela & M. A. Blasco, personal communication). Furthermore, cell immunostaining with annexin V and propidium iodide, or immunohistochemical analysis of activated caspase-3 levels, did not reveal major differences between

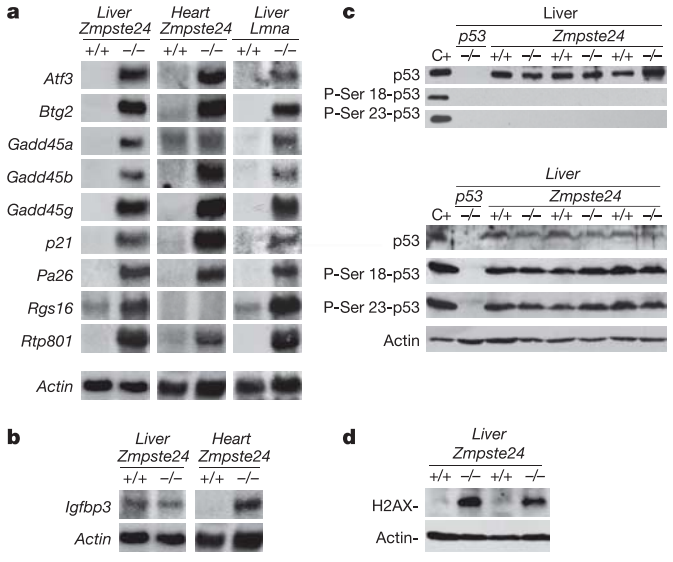

Figure 1 | Activation of a p53-induced pathway as a result of *Zmpste24* or *Lmna* deficiencies. **a**, Northern blot analysis of p53 targets in liver (left panel) and heart (middle panel) from *Zmpste24*$^{-/-}$ mice, and in liver from *Lmna*$^{-/-}$ mice (right panel). **b**, Northern blot showing *Igfbp3* overexpression in heart but not in liver from *Zmpste24*$^{-/-}$ mice. **c**, Top panel: western blot analysis of p53 immunoprecipitated from *Zmpste24*$^{-/-}$ and control livers. Doxorubicin-treated mouse fibroblasts and *p53*-deficient liver extracts were used as positive and negative controls, respectively. Bottom panel: western blot analysis of liver extracts from γ-irradiated *Zmpste24*$^{-/-}$ and control mice. **d**, Western blot analysis of phosphorylated histone H2AX in liver extracts from severely affected *Zmpste24*$^{-/-}$ mice and age-matched controls.

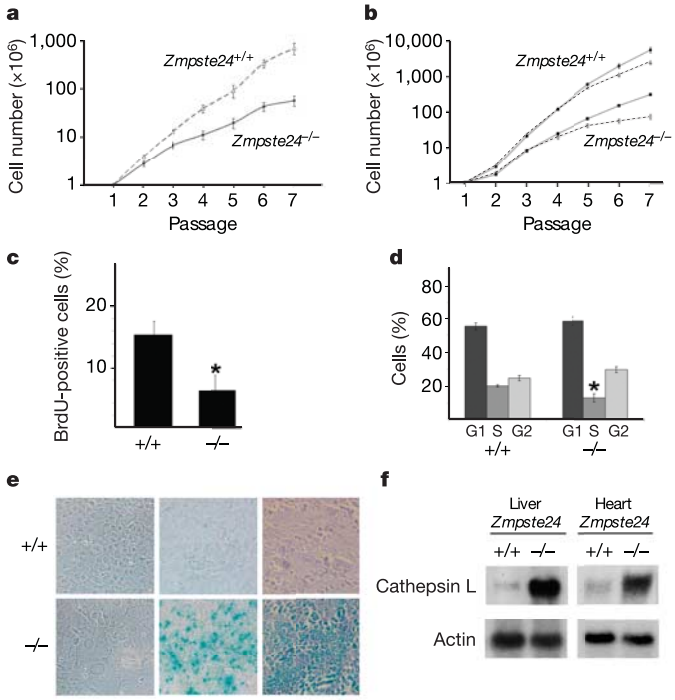

Figure 2 | Senescence in *Zmpste24*$^{-/-}$ mice **a**, Proliferation assay of adult fibroblasts from *Zmpste24*$^{-/-}$ ($n = 8$) and control mice ($n = 7$). **b**, Proliferation assay of fibroblasts from three wild-type and three *Zmpste24*$^{-/-}$ mice, cultured under atmospheric (20%, dashed lines) and reduced (3%, solid lines) oxygen concentrations. **c**, BrdU incorporation in fibroblasts of *Zmpste24*$^{-/-}$ ($n = 2$) and control ($n = 2$) mice at passage 2. **d**, Cell cycle analysis of control ($n = 3$) and *Zmpste24*$^{-/-}$ ($n = 3$) fibroblasts at passage 3. **e**, Flattened and enlarged morphology of *Zmpste24*$^{-/-}$ adult fibroblasts at passage 6 (left panel). Senescence-associated β-galactosidase assay of passage 6 adult fibroblasts (middle panel) and kidneys (right panel) from control and *Zmpste24*$^{-/-}$ mice. **f**, Northern blot analysis of cathepsin L expression in liver and heart from *Zmpste24*$^{-/-}$ and control mice. Error bars represent s.e.m.; asterisk indicates $P < 0.05$.

samples from mutant and control mice (Supplementary Fig. 5 and data not shown). Therefore, increased apoptosis does not have a major role in the observed reduction of the proliferative activity of mutant fibroblasts. Taken together, these data suggest that a p53-linked response to the persistent nuclear abnormalities of *Zmpste24*$^{-/-}$ mice would cause a loss of their normal cell function mainly through activation of a senescence-like programme. The progressive decline in tissue-specific functions, probably derived from the activation of this cellular programme, would then contribute to the premature ageing phenotype exhibited by these *Zmpste24*-null mice.

The above results prompted us to hypothesize that targeting either the accumulated prelamin A or the p53 signalling pathway triggered by the nuclear envelope defects of *Zmpste24*$^{-/-}$ mice could rescue the multiple abnormalities occurring in these mice. In relation to the first possibility, it has been reported that heterozygous *Lmna*$^{+/-}$ mice do not show apparent abnormalities[4], which led us to speculate that generation of *Zmpste24*$^{-/-}$*Lmna*$^{+/-}$ mice would decrease prelamin A levels without generating additional defects to those derived from the protease deficiency itself. Notably, *Zmpste24*$^{-/-}$*Lmna*$^{+/-}$ mice exhibit a total recovery of all progeroid phenotypes observed in *Zmpste24*-null mice (Fig. 3). During preparation of this manuscript, similar findings have been reported in another strain of *Zmpste24*$^{-/-}$ mice[23]. Similarly, western blot analysis revealed a strong reduction of both prelamin A and lamin C protein levels in *Zmpste24*$^{-/-}$*Lmna*$^{+/-}$ mice (Fig. 3). This reduction is accompanied by a recovery of the normal shape in *Zmpste24*$^{-/-}$*Lmna*$^{+/-}$ nuclei (Supplementary Fig. 4). Histopathological analysis also confirmed that the appreciable defects present in tissues from *Zmpste24*$^{-/-}$ mice were absent in *Zmpste24*$^{-/-}$*Lmna*$^{+/-}$ mice. Finally, no evidence of cell senescence or induction of p53 targets was found in *Zmpste24*$^{-/-}$*Lmna*$^{+/-}$ mice (Fig. 3 and data not shown).

To explore the possibility that the progeroid defects of *Zmpste24*$^{-/-}$ mice could also be rescued by targeting the abnormally activated p53 signalling pathway, we generated *Zmpste24*$^{-/-}$*p53*$^{-/-}$ mice. These mice show a partial recovery of the phenotype characteristic of the Zmpste24 deficiency and exhibit a marked gain of weight and an increased lifespan (Fig. 4). We next examined whether the absence of p53 could also result in a recovery of the cell senescence features observed in *Zmpste24*$^{-/-}$ mice. As shown in Fig. 4, fibroblasts from *Zmpste24*$^{-/-}$*p53*$^{-/-}$ mice do not show the reduced proliferative capacity observed in *Zmpste24*$^{-/-}$ cells. Moreover, no senescence-

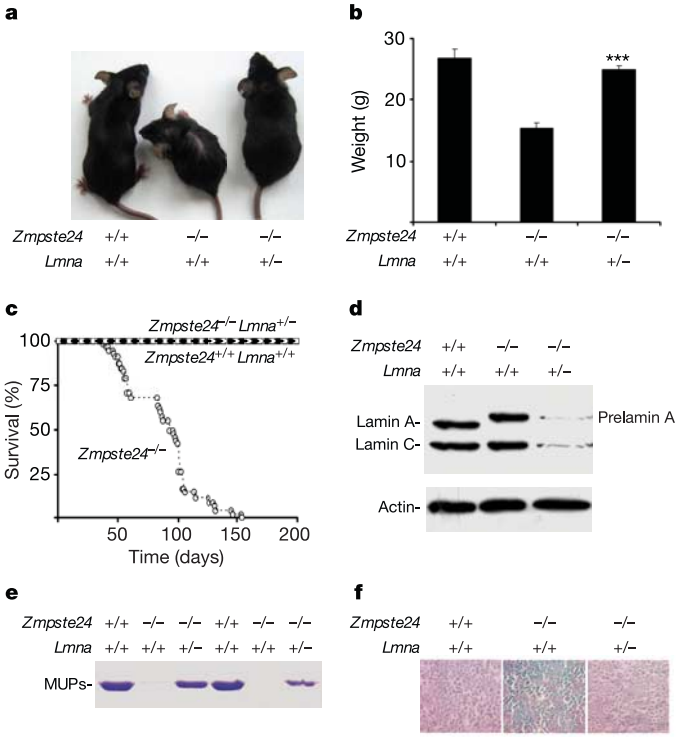

Figure 3 | *Lmna* heterozygosity rescues the *Zmpste24*$^{-/-}$ phenotype. **a**, Photograph of 4-month-old *Zmpste24*$^{+/+}$*Lmna*$^{+/+}$, *Zmpste24*$^{-/-}$*Lmna*$^{+/+}$ and *Zmpste24*$^{-/-}$*Lmna*$^{+/-}$ mice. **b**, Body weight of 3-month-old *Zmpste24*$^{+/+}$*Lmna*$^{+/+}$ ($n = 9$), *Zmpste24*$^{-/-}$*Lmna*$^{+/+}$ ($n = 10$) and *Zmpste24*$^{-/-}$*Lmna*$^{+/-}$ ($n = 17$) mice. **c**, Kaplan–Meier graph of *Zmpste24*$^{+/+}$*Lmna*$^{+/+}$ ($n = 7$) and *Zmpste24*$^{-/-}$*Lmna*$^{+/-}$ ($n = 7$) mice. The survival curve of *Zmpste24*$^{-/-}$ mice is also shown ($n = 45$). **d**, Western blot analysis of lamins A and C in extracts from *Zmpste24*$^{+/+}$*Lmna*$^{+/+}$, *Zmpste24*$^{-/-}$*Lmna*$^{+/+}$ and *Zmpste24*$^{-/-}$*Lmna*$^{+/-}$ adult fibroblasts. **e**, SDS–PAGE of urine from *Zmpste24*$^{+/+}$*Lmna*$^{+/+}$, *Zmpste24*$^{-/-}$*Lmna*$^{+/+}$ and *Zmpste24*$^{-/-}$*Lmna*$^{+/-}$ male mice, showing recovery of production of major urinary proteins (MUPs). **f**, Senescence-associated β-galactosidase assay in kidney. Error bars represent s.e.m.; triple asterisk indicates $P < 0.001$.

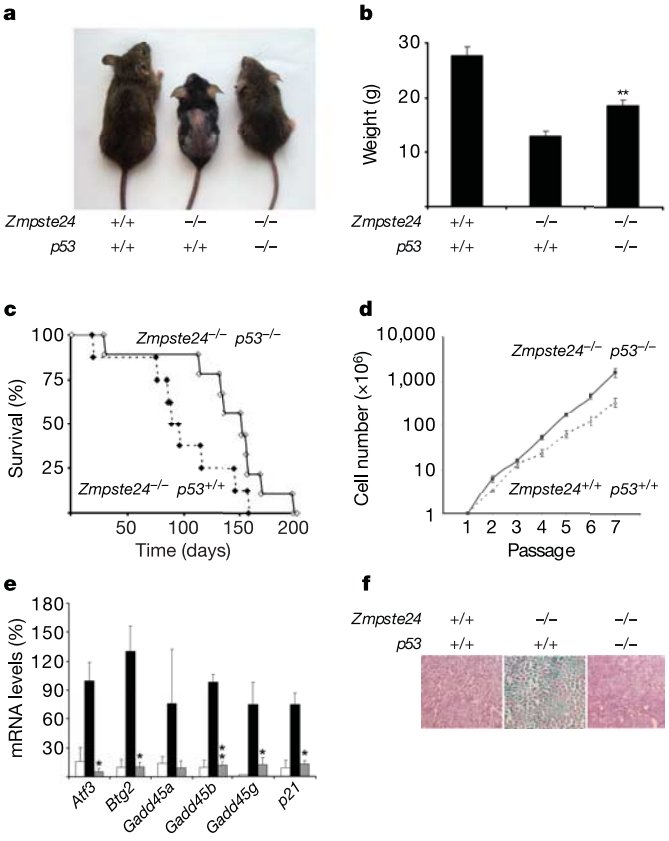

Figure 4 | Partial recovery of the *Zmpste24*$^{-/-}$ phenotype in a p53-null background. **a**, Representative photograph of 3-month-old *Zmpste24*$^{+/+}$*p53*$^{+/+}$, *Zmpste24*$^{-/-}$*p53*$^{+/+}$ and *Zmpste24*$^{-/-}$*p53*$^{-/-}$ littermates. **b**, Total body weight of 3-month-old *Zmpste24*$^{+/+}$*p53*$^{+/+}$ ($n = 14$), *Zmpste24*$^{-/-}$*p53*$^{+/+}$ ($n = 6$) and *Zmpste24*$^{-/-}$*p53*$^{-/-}$ ($n = 9$) mice. **c**, Kaplan–Meier survival graph of *Zmpste24*$^{-/-}$*p53*$^{+/+}$ ($n = 8$) and *Zmpste24*$^{-/-}$*p53*$^{-/-}$ ($n = 9$) mice. **d**, Proliferation assay of adult fibroblasts from control and *Zmpste24*$^{-/-}$*p53*$^{-/-}$ mice. **e**, Transcriptional analysis by real-time quantitative PCR of p53 targets (and related genes) in grossly affected 3-month-old *Zmpste24*$^{-/-}$*p53*$^{+/+}$ (black bars) ($n = 3$) mice and age-matched *Zmpste24*$^{+/+}$*p53*$^{+/+}$ (white bars) ($n = 3$) and *Zmpste24*$^{-/-}$*p53*$^{-/-}$ (grey bars) ($n = 3$) mice. mRNA levels are expressed as per cent values relative to a pool of *Zmpste24*$^{-/-}$ liver RNAs. **f**, Senescence-associated β-galactosidase assay in kidney. Error bars represent s.e.m.; asterisk indicates $P < 0.05$; double asterisk indicates $P < 0.01$.

associated β-galactosidase staining was detected in kidneys from these double mutant mice. Lastly, quantitative PCR analysis of RNA levels of p53 targets in liver from severely affected *Zmpste24*$^{-/-}$*p53*$^{+/+}$ and age-matched *Zmpste24*$^{-/-}$*p53*$^{-/-}$ mice revealed decreased levels of *p21*, *Btg2*, *Gadd45a*, *Gadd45b*, *Gadd45g* and *Atf3* in the double knockout mice when compared with *Zmpste24*$^{-/-}$*p53*$^{+/+}$ animals (Fig. 4). Taken together, these results demonstrate that the absence of p53 rescues some molecular alterations observed in *Zmpste24*$^{-/-}$ mice. However, the fact that the multiple *Zmpste24*$^{-/-}$ phenotype alterations were not rescued in a *p53*-null background to the same extent as in the case of the *Lmna*$^{+/-}$ background indicates that other pathways contribute to the generation of the observed defects. In this regard, and consistent with previous findings in *Lmna*$^{-/-}$ mice[24], it is of interest that retinoblastoma protein levels are reduced in *Zmpste24*$^{-/-}$ mice (Supplementary Fig. 6). The microarray analysis also revealed changes in expression levels of a series of genes that were not described as p53 targets but that are of putative relevance for the observed phenotype in *Zmpste24*-null mice. This is the case for CD14 (upregulated 26-fold in the liver of *Zmpste24*$^{-/-}$ mice), a receptor involved in apoptotic cell removal, the protein kinase Pim-3 (upregulated 13-fold), and the peroxisomal catalase (downregulated 6.1-fold) (Supplementary Table 1). Interestingly, levels of this antioxidant enzyme are reduced in fibroblasts of Hutchinson–Gilford progeria patients[25], its genetic ablation causes a progeric phenotype in *Caenorhabditis elegans*[26], and its overexpression extends murine lifespan[27]. Therefore, the low levels of peroxisomal catalase in *Zmpste24*$^{-/-}$ mice could contribute to the generation of some of the progeroid features observed in these mutant mice. Further studies will be required to identify the additional pathways that can cooperate with p53 in the generation of the multiple defects caused by accumulation of prelamin A in *Zmpste24*$^{-/-}$ mutant mice. These studies may also provide additional information on the relevance, in both normal and pathological conditions, of the herein reported links between p53—the guardian of the genome—and lamin A—the guardian of the soma[18,28].

These phenotype rescue experiments support the conclusion that prelamin A accumulation in the nuclear envelope is the initial molecular event responsible for most or all phenotypic alterations, including progeroid features, observed in *Zmpste24*$^{-/-}$ mice. These nuclear lamina alterations induce chromatin architecture changes that influence the regulation of gene expression through different signalling pathways, including those mediated by p53 activation. The finding of a p53 response linked to the activation of a cell senescence programme in *Zmpste24*$^{-/-}$ progeroid mice could provide a connection of this model to recent work showing that mice producing a hyperactive p53 mutant protein or overexpressing a short isoform of p53 also exhibit accelerated ageing[11,29]. Our results should also be consistent with the occurrence of a structural checkpoint that examines the integrity of the nuclear envelope and responds to putative damages in this structure by activating archetypal DNA damage responses such as those mediated by p53. Finally, the finding that the progeroid phenotypes in *Zmpste24*$^{-/-}$ mice can be largely or partially rescued by lowering prelamin A levels or by targeting the p53 pathway activated by prelamin A accumulation, suggests that similar strategies might provide some therapeutic benefit to patients suffering from these devastating diseases.

METHODS

Animals. *Zmpste24*-deficient mice and *Lmna*-deficient mice were generated and genotyped as described[1,4]. *p53*-deficient mice[30] were provided by M. Serrano. Hepatic DNA damage was induced in 3-month-old mice by exposition to a single dose (10 Gy) of whole-body γ-irradiation. Animal experimentation was done in accordance with the guidelines of the Universidad de Oviedo.

Transcriptional profiling. Total RNA was isolated using an RNeasy kit (Qiagen). Double-stranded cDNA was synthesized using the SuperScriptTM cDNA synthesis kit (Invitrogen). *In vitro* transcription was carried out with the Bioarray high yield RNA transcript labelling kit (Enzo Diagnostics). The biotin-labelled cRNA was purified, fragmented and hybridized to murine genome U74Av2 GeneChips (Affymetrix).

Real-time quantitative PCR. Expression levels of selected genes (*Atf3*, *Btg2*, *Gadd45a*, *Gadd45b*, *Gadd45g* and *p21*) were analysed by using Applied Biosystems Taqman gene expression assays in an ABI7000 Sequence detection system (Applied Biosystems) following the manufacturer's instructions.

Western blotting and immunoprecipitation. Liver samples were homogenized in 50 mM Tris (pH 7.4), 150 mM NaCl, 1% NP-40, 50 mM NaF, 1 mM dithiothreitol, 2 mg ml^{-1} pepstatin A, Complete inhibitor cocktail (Roche) and phosphatase inhibitor cocktails I and II (Sigma). p53 immunoprecipitation was performed with anti-p53 goat polyclonal antibody (FL-393-G, Santa Cruz). Immunoprecipitates were electrophoresed and transferred to nitrocellulose membranes. Blots were blocked with 3% non-fat dry milk, and incubated overnight at 4 °C with 1/5,000 anti-p53 rabbit polyclonal antibody CM1 (a gift of S. Laín), 1/100 anti-pRb (sc-102, Santa Cruz), 1/100 anti-p21 (sc-6246, Santa Cruz), 1/500 anti-laminA/C (MANLAC1, a gift from G. Morris), 1/100 anti-phosphohistone H2AX (05-636, Upstate), and 1/10,000 anti-β-actin (A5441, Sigma). Finally, blots were incubated with 1/1,000 goat anti-rabbit-HRP (Pierce) or 1/2,000 of anti-mouse-HRP (Amersham) in 1.5% non-fat milk, washed and developed with Femto chemiluminescent reagent (Pierce). To analyse levels of phosphorylated p53, membranes used to quantify total p53 were stripped and incubated with 1/1,000 rabbit polyclonal anti-phosphoserine-p53 (Ser 15)- or anti-phosphoserine-p53 (Ser 20)-specific antibodies (Cell Signaling).

Cell culture and proliferation assays. Fibroblasts were extracted from the ears of 12-week-old mice. Ears were sterilized with ethanol, washed with PBS and triturated with razor blades. Samples were then incubated with 600 μl of 4 mg ml^{-1} collagenase D (Roche) and 4 mg ml^{-1} dispase II (Roche) in DMEM (Invitrogen) for 45 min at 37 °C and 5% CO_2. After filtering and washing, 6 ml of DMEM with 10% FBS (Invitrogen) and 1% antibiotic-antimycotic (Invitrogen) were added, and the mixture was incubated at 37 °C and 5% CO_2. 10^6 cells were passed in a 10-cm plate every 3 days and cultured in 3% or 20% oxygen. To measure BrdU incorporation, cells were incubated for 4 h with 100 μg μl^{-1} BrdU (Sigma), fixed with paraformaldehyde, and immunofluorescence was carried out with the B2531 antibody (Sigma).

Cell senescence and apoptosis assays. Senescence-associated β-galactosidase assays were carried out as described[19]. Apoptotic cells were measured with annexin-V FITC (BD Pharmigen) by flow cytometry. Immunohistochemical analyses were carried out in formalin-fixed tissues with anti-cleaved caspase-3 antibody (Cell Signaling).

Received 19 May; accepted 20 July 2005.
Published online 3 August 2005.

1. Pendás, A. M. *et al.* Defective prelamin A processing and muscular and adipocyte alterations in Zmpste24 metalloproteinase-deficient mice. *Nature Genet.* **31,** 94–99 (2002).
2. Bergo, M. O. *et al.* Zmpste24 deficiency in mice causes spontaneous bone fractures, muscle weakness, and a prelamin A processing defect. *Proc. Natl Acad. Sci. USA* **99,** 13049–13054 (2002).
3. Corrigan, D. P. *et al.* Prelamin A endoproteolytic processing *in vitro* by recombinant Zmpste24. *Biochem. J.* **387,** 129–138 (2005).
4. Sullivan, T. *et al.* Loss of A-type lamin expression compromises nuclear envelope integrity leading to muscular dystrophy. *J. Cell Biol.* **147,** 913–920 (1999).
5. Mounkes, L. C., Kozlov, S., Hernandez, L., Sullivan, T. & Stewart, C. L. A progeroid syndrome in mice is caused by defects in A-type lamins. *Nature* **423,** 298–301 (2003).
6. Agarwal, A. K., Fryns, J. P., Auchus, R. J. & Garg, A. Zinc metalloproteinase, ZMPSTE24, is mutated in mandibuloacral dysplasia. *Hum. Mol. Genet.* **12,** 1995–2001 (2003).
7. De Sandre-Giovannoli, A. *et al.* Lamin a truncation in Hutchinson-Gilford progeria. *Science* **300,** 2055 (2003).
8. Eriksson, M. *et al.* Recurrent de novo point mutations in lamin A cause Hutchinson-Gilford progeria syndrome. *Nature* **423,** 293–298 (2003).
9. Chen, L. *et al.* LMNA mutations in atypical Werner's syndrome. *Lancet* **362,** 440–445 (2003).
10. Navarro, C. L. *et al.* Loss of ZMPSTE24 (FACE-1) causes autosomal recessive restrictive dermopathy and accumulation of Lamin A precursors. *Hum. Mol. Genet.* **14,** 1503–1513 (2005).
11. Tyner, S. D. *et al.* p53 mutant mice that display early ageing-associated phenotypes. *Nature* **415,** 45–53 (2002).
12. Yu, J. *et al.* Identification and classification of p53-regulated genes. *Proc. Natl Acad. Sci. USA* **96,** 14517–14522 (1999).
13. Qiu, W. *et al.* Hypermethylation of growth arrest DNA damage-inducible gene 45 beta promoter in human hepatocellular carcinoma. *Am. J. Pathol.* **165,** 1689–1699 (2004).
14. Fei, P., Bernhard, E. J. & El-Deiry, W. S. Tissue-specific induction of p53 targets *in vivo*. *Cancer Res.* **62,** 7316–7327 (2002).

15. Wei, W., Hemmer, R. M. & Sedivy, J. M. Role of p14(ARF) in replicative and induced senescence of human fibroblasts. *Mol. Cell. Biol.* **21,** 6748–6757 (2001).
16. Bode, A. M. & Dong, Z. Post-translational modification of p53 in tumorigenesis. *Nature Rev. Cancer* **4,** 793–805 (2004).
17. Liu, B. *et al.* Genomic instability in laminopathy-based premature aging. *Nature Med.* **11,** 780–785 (2005).
18. Vogelstein, B., Lane, D. & Levine, A. J. Surfing the p53 network. *Nature* **408,** 307–310 (2000).
19. Dimri, G. P. *et al.* A biomarker that identifies senescent human cells in culture and in aging skin *in vivo*. *Proc. Natl Acad. Sci. USA* **92,** 9363–9367 (1995).
20. Campisi, J. Cancer and ageing: rival demons? *Nature Rev. Cancer* **3,** 339–349 (2003).
21. Serrano, M. & Blasco, M. A. Putting the stress on senescence. *Curr. Opin. Cell Biol.* **13,** 748–753 (2001).
22. Sharpless, N. E. & DePinho, R. A. Telomeres, stem cells, senescence, and cancer. *J. Clin. Invest.* **113,** 160–168 (2004).
23. Fong, L. G. *et al.* Heterozygosity for Lmna deficiency eliminates the progeria-like phenotypes in Zmpste24-deficient mice. *Proc. Natl Acad. Sci. USA* **101,** 18111–18116 (2004).
24. Johnson, B. R. *et al.* A-type lamins regulate retinoblastoma protein function by promoting subnuclear localization and preventing proteasomal degradation. *Proc. Natl Acad. Sci. USA* **101,** 9677–9682 (2004).
25. Yan, T., Li, S., Jiang, X. & Oberley, L. W. Altered levels of primary antioxidant enzymes in progeria skin fibroblasts. *Biochem. Biophys. Res. Commun.* **257,** 163–167 (1999).
26. Petriv, O. I. & Rachubinski, R. A. Lack of peroxisomal catalase causes a progeric phenotype in *Caenorhabditis elegans*. *J. Biol. Chem.* **279,** 19996–20001 (2004).
27. Schriner, S. E. *et al.* Extension of murine lifespan by overexpression of catalase targeted to mitochondria. *Science* **308,** 1909–1911 (2005).
28. Hutchison, C. J. & Worman, H. J. A-type lamins: guardians of the soma? *Nature Cell Biol.* **6,** 1062–1067 (2004).
29. Maier, B. *et al.* Modulation of mammalian life span by the short isoform of p53. *Genes Dev.* **18,** 306–319 (2004).
30. Jacks, T. *et al.* Tumor spectrum analysis in p53-mutant mice. *Curr. Biol.* **4,** 1–7 (1994).

Supplementary Information is linked to the online version of the paper at www.nature.com/nature.

Acknowledgements We thank A. Astudillo for help with histopathological analysis; E. Fermiñán (CIC-Salamanca) for help with microarray experiments; X. S. Puente, A. Fueyo, J. Alvarez, P. Zuazua, G. Velasco, A. Bernad, S. Laín and M. Serrano for support and comments; T. Sánchez and L. Santos for help in animal care facilities; and M. Fernández, S. Alvarez and M. S. Pitiot for technical assistance. This work was supported by grants from Ministerio de Educación y Ciencia, Fundación "La Caixa", the European Union, the Swedish Research Council, the Swedish Cancer Society and the Research Grant Council of Hong Kong. The Instituto Universitario de Oncología is supported by Obra Social Cajastur, and Red de Centros de Cancer Instituto Carlos III, Spain.

Author Information Reprints and permissions information is available at npg.nature.com/reprintsandpermissions. The authors declare no competing financial interests. Correspondence and requests for materials should be addressed to C.L.-O. (clo@uniovi.es).